

Reference : Aerodynamics AE 03

## ***A Study of Helicopter Tail Rotor Interaction:***

### ***Phase 1 - Proof of Concept***

C.M. Copland, F.N. Coton, R.A.McD. Galbraith

Department of Aerospace Engineering,  
The University of Glasgow,  
Glasgow, G12 8QQ  
Scotland

This paper describes the design, development and initial testing of a new facility for the generation of transverse vortices for use in a wind tunnel based study of helicopter tail rotor blade-vortex interaction. The facility consists of a single-bladed pitching rotor, positioned in the contraction of a low speed wind tunnel, which generates a transverse vortex representative of the idealised vortex system associated with a rotor blade. The manner in which a numerical model was utilised during the design process, to provide an accurate means of determining design parameters such as vortex generator position, rotational speed, working section velocity and blade pitch profile, is described. Initial hot-wire measurements, which were made downstream of the generator and document the periodic motion of the convecting vortex structure, are also presented. Finally, the remaining stages of the research programme are outlined.

#### ***Introduction***

The interactional aerodynamics of tail rotors have been minimally researched in comparison to those of main rotors<sup>1,2,3</sup>. There is, consequently, a universal lack of understanding of the many interactional mechanisms that affect helicopter tail rotor performance. Inevitably, there are significant differences between interactions where the vortex path lies in, or close to, the plane of the main rotor blade (Fig. 1), i.e. the common conception of Blade Vortex Interaction (BVI), and interactions associated with the tail rotor environment where the vortex is orthogonal to the tail rotor blade (Fig. 2).

Despite the importance of BVI being recognised for many years<sup>4,7</sup> and being the focus of several experimental<sup>8-14</sup> and numerical<sup>15,16</sup> studies, very few studies have investigated tail rotor interactional effects. Possibly the most notable was the in-flight study of Ellin<sup>1</sup>, which considered the interaction of the main rotor wake with the tail rotor for a range of flight conditions. Ellin stated that the isolated convecting main rotor vortex can interact with the tail rotor itself (Fig. 2. Position 1), or with its wake both during the roll-up of the trailing tail rotor tip vortex (Fig. 2. Position 2) and with the fully rolled up tip vortex (Fig. 2. Position 3).

Unfortunately, there is no apparent work documented on the specific mechanisms that are associated with these particular phenomena.

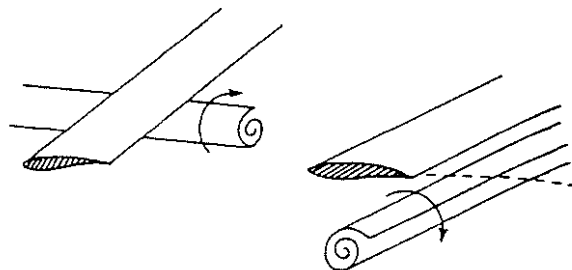


**Fig.1- Illustration of the vortical flow field associated main rotor BVI.**

It is well known that a helicopter in forward flight can generate a flow field similar to that of a fixed wing aircraft (Fig. 3). These vortices are generated from the individual blade tip vortices rolling around each other to form larger trailed structures. In addition to these structures, a series of connecting transverse tip vortex segments are produced by the passage of the rotor blades around the forward and aft regions of the rotor disk. Thus, in forward flight the tail rotor will be in the centre of the main rotor wake and will cut each of these transverse vortex segments in sequence as they are trailed

from the rear of the disc. In quartering flight (Fig. 4), however, the tail rotor can become immersed in the large rolled up vortex structures trailed from the edge of the main rotor disc. This flight condition has the most significant effect on tail

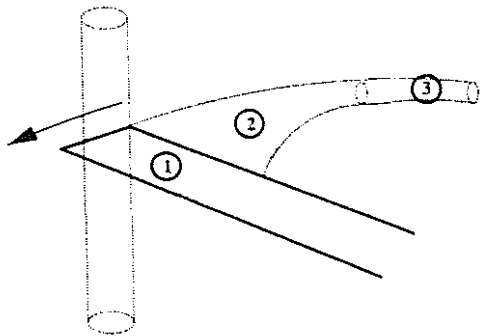


**Fig.2-** Illustration of the vortical flow field associated with tail rotor BVI.

rotor performance. Depending on the relative rotation of the vortices and tail rotor, the net effect can be a dramatic loss in tail rotor performance.

It is well known that the direction of the rotor rotation, the type (pusher or puller) and the position relative to the main rotor disk, all have a significant effect on tail rotor performance. It is likely that all these design factors are related to the interaction with the main rotor tip vortices and wake. It is not understood why this is the case. The evolution of a specific helicopter tail rotor design has followed a trial and error approach but the general consensus is top blade forward gives the best tail rotor performance. In many cases it is only when the yaw handling of a helicopter is unsatisfactory that research has been carried out<sup>17</sup>. Although understanding of the tail rotor has improved over the years, the fundamental orthogonal interactions are still not understood.

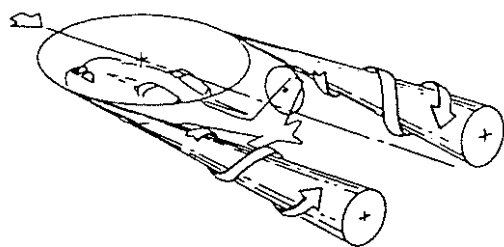


**Fig.3-** Illustration of the flow field associated with a helicopter in forward flight.

In his study, Ellin concluded that the furtherance of the understanding of main rotor/tail rotor interactions would benefit from two particular areas of research;

- 1) An experimental investigation of interactions where the vortex is orthogonal to the blade leading edge

- 2) An experimental investigation of blade vortex interaction with the vortex perpendicular to the blade chord.

This paper documents the first stage of a research programme to address the latter of these two topics and goes on to describe the remaining stages of the programme.

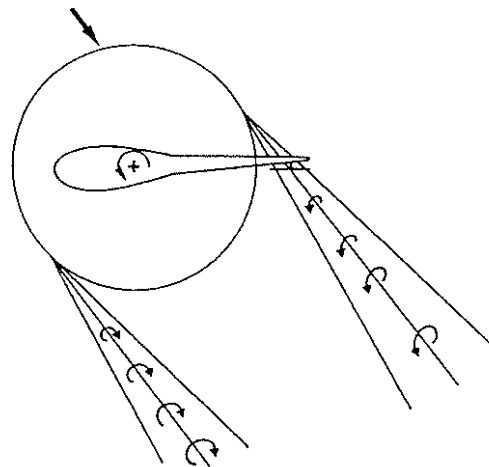


**Fig.4-** Illustration of a helicopter in quartering flight.

Previous experimental studies of main rotor BVI have been predominantly wind tunnel based and have utilised a variety of test geometry's to create the BVI phenomenon. Early studies attempted to isolate single interactions in the hope that a clear description of the process would be forthcoming. Unfortunately, these tests were often hampered by problems associated with vortex generation or poor measurement resolution. In recent years, improvements in instrumentation technology have allowed more detailed studies of BVI, both as an isolated phenomenon and also in the full rotor domain to be conducted. In the surface pressure measurement and flow visualisation work of Homer et al.<sup>12,13,14</sup> a vortex generator was located upstream of a single-bladed rotor in the working section of a low-speed wind tunnel. During the interaction of the vortex with the rotor blade, unsteady surface pressures were measured and Particle Image Velocimetry was used to obtain quantitative flow field information.

Other studies have used different experimental set-ups to investigate the fundamental aspects of blade vortex interactions. Booth et al.<sup>8,9,10</sup> utilised an oscillating aerofoil to generate transverse vortices. However, the wake behind the aerofoil contained pairs of vortices which resembled a Karman vortex street. It was pointed out that there are some inherent limitations in this experimental method. Firstly, the vortex pairs cannot be considered to be exactly equivalent to an isolated tip vortex encountering a rotor blade on a

helicopter. Since the vortices occur in pairs, they influence each other. Secondly, in the presence of a blade, the spacing between the filaments becomes important. The blade can be said to have an isolated encounter only if the spacing between the vortices is greater than the blade model chord. Such a requirement may conflict with the need for a well defined vortex and consequently the condition for an isolated encounter is not always met.

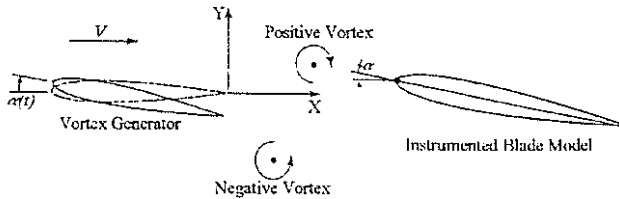


**Fig.5- Illustration of the vortex system associated with an oscillating wing (Ref.8)**

Straus et al. utilised a similar facility to Booth but limited the pitching motion to a single ramp up profile rather than a continuously oscillating motion. The aerofoil was rapidly pitched to try and obtain a single two-dimensional shed vortex. However, as stated by Straus, the response time of the pitching system is crucial to produce a single rolled-up shed vortex. The required time of motion of the pitching aerofoil should be less than the time it takes the air to travel one chord length. If the time is too long the shed vorticity will not roll-up into the required vortex. As expected, at low velocities the time to pitch the aerofoil is short - a threshold time of 21ms is quoted at a freestream velocity of 12.2 m/s. However, if the freestream velocity were to be increased, the threshold time to attain a single vortex would decrease and so mechanical actuation limits may be reached which could limit the operational range of the generator. Flow separation may also occur which could result in the generation of another vortex of opposite sense to the original shed vortex. It is also difficult to vary the size and strength of the generated vortex.

It may, therefore, be concluded that the crucial factor in all experiments to date has been the manner in which the interacting vortices have been generated and their subsequent trajectory through the wind tunnel's working section. These two features are of critical importance in interpreting the resultant data collected and in the application of such interpretations to real aircraft. When data pertaining to blade vortex interactions are acquired from experiments in which the generation of the interacting vortex differs, there are clear differences in the flow development. How important these differences are is not clear, and it may be that they simply affect the peripheral response and not the fundamental interaction. Nonetheless, whatever system is used, it is

essential that the detailed structure of the interacting vortex is known. It is also important to have a good knowledge of the vortex trajectory, stability and tendency to wander from its mean path. This applies irrespective of the method of generation.

To mimic the convection of a main rotor tip vortex requires the generation of a transverse vortex which will travel in a stable fashion through the wind tunnel's working section. As discussed previously, the conventional generation method for such a vortex is to place an aerofoil at the entrance of the working section and subject it to a rapid change in incidence. Although this procedure is fraught with difficulty, it does produce a vortex, but one in which the structure may not comprehensively mimic the trailing vortex from the tip of a rotor. Accordingly, it was decided to investigate the generation of a tip vortex via the alternative method of a rotor placed in the settling chamber of a wind tunnel. The first stage of the present study was to establish the feasibility of this method of vortex generation.

This paper examines the method of generation and subsequent behaviour of a transverse vortex in a wind tunnel environment. The initial parametric design of the vortex generator, using a numerical model, is presented along with the mechanical design of the facility. Preliminary results, obtained using hot-wire anemometry, which document both the clarity of the vortex structure and its downstream movement are also presented and discussed. Finally, the remaining phases of the experimental programme, which are currently underway, are outlined.

### **Numerical Modelling**

To aid in the experimental design, development and verification of the experimental facility, it was initially decided to model the convecting vortex numerically. This model was then used to determine design parameters for the subsequent manufacture of the test facility.

The transverse vortex was to be produced by a rotating blade placed in the contraction a low speed wind tunnel. This configuration posed a number of complex problems that could only be overcome with the aid of the numerical model. The first, and most significant problem, was the accelerating flow field associated with the contraction of the tunnel. This had to be modelled to determine the effect of the velocity gradient on the convecting tip vortex and wake.

Also of interest at this stage were the relevant geometrical parameters of the blade, and the operating conditions of the blade and wind tunnel,

to attain a good representation of a transverse vortex. The developed code, therefore, had to be adaptable to enable a comprehensive analysis of the fundamental input parameters such as position, size and motion of the blade, and working section velocity. Results had to illustrate the three dimensional development of the wake (and related tip vortex) through the wind tunnel with enough clarity to isolate the specific effects of a particular design parameter.

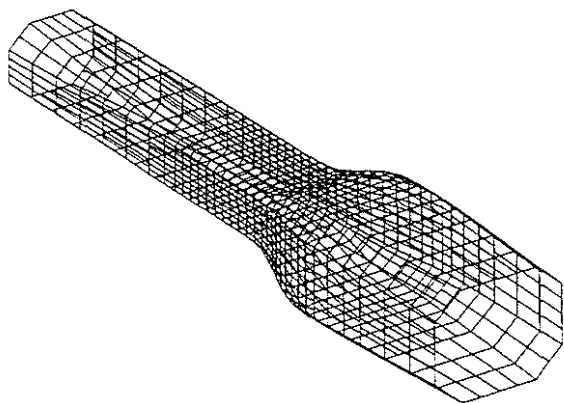


**Fig.6- Illustration of the discretised tunnel geometry used as input to the 3 dimensional panel method.**

The features of the experimental facility that had to be modelled were the vortical wake structure generated from the rotating blade and the main flow through the wind tunnel. The rotor wake was represented by a free wake vortex model consisting of a lattice of shed and trailed vortex elements which were generated using classical lifting line theory. This vortex system was then convected through the contraction and working section of the wind tunnel with the superposition of the local velocity, calculated via a three dimensional source panel method, and the induced velocity components from the vortex elements. Due to the inviscid nature of this model, no account was taken of vortex dissipation or the change in vortex strength due to deformation of the vortex element, and so the strength of each vortex element was invariant with time.

A source panel method was used to represent the constraining effects of the wind tunnel walls. The method adopted was based on the work of Hess and Smith and was chosen for its relative simplicity and adaptability to internal flows. Due to the simple geometry of the modelled portion of the wind tunnel and the non-lifting nature of the body, it was deemed sufficient to represent the wall surfaces using plane quadrilateral elements with constant source distributions.

The internal surface of the wind tunnel was discretised into approximately 1000 individual

quadrilateral elements representing the settling chamber, contraction, working section and diffuser (Fig.6). This representation gave sufficient distance upstream of the vortex generator location to be out of its disturbance environment, and extended far enough downstream to allow the vortex system to convect through and out of the working section. Since the accuracy of such calculations can depend not only on the number of quadrilateral elements used but also on the manner in which these elements are distributed over the surface, a non-uniform distribution of panels was used. In particular, panels were concentrated in the region of the contraction (area of high curvature) and the working section (area of interest).

The panel method and the wake model were loosely coupled in that the induced velocities from the wake were not taken into account when calculating the source strengths of the panels. This was done for efficiency since strongly linking the two models, by calculating the induced velocities from the wake at each panel collocation point, would have significantly increased the computational time and so limited the range of cases which could have been considered in the parametric study. This approach was considered acceptable due to the low blockage presented by the generator assembly.

### ***Parametric Design Study***

Two possible operating strategies were investigated for the vortex generator. Both involved the blade undergoing a specified variation in pitch angle with azimuth position. The intention was to have zero pitch on the upwind pass of the blade and then a variation of pitch angle on the downwind pass where the desired vortex structure would be produced. The aim was to produce an interacting vortex whose strength was as constant as possible along its length.

The first operating strategy involved the rotating blade accelerating from rest up to a specified speed and then being returned to rest; all within one rotor rotation. This had the advantage of producing one clean vortex structure which could be very carefully controlled by variations in rotational velocity and pitch profile.

The alternative strategy was to use a blade rotating continuously at constant speed. This approach did not require the complicated motion profiles of the single rotation cases. In fact, with the blade operating at constant rotational speed, only a pitch variation has to be specified. It is worthy of note that, while the blade traverses the area ahead of the working section, the magnitude of the normal velocity component on the blade from the tunnel flow is small compared to that of

the rotating blade itself. Hence, it is appropriate to conclude that with an almost constant tip velocity profile in this region, a constant pitch incidence would be acceptable to attain (approximately) a constant tip vortex strength.

Preliminary analysis indicated that the wind tunnel velocity, the blade rotational speed, and the position of the hub axis primarily determine the wake geometry. The relative magnitudes of the tunnel velocity and the rotational speed determine the extent to which the wake is skewed and, in the continuous running case, the separation between each consecutive convecting wake structure. The rotor hub position, on the other hand, dictates the wake curvature and elongation. For the latter, it is important for the blade to be positioned close to the working section to minimise vortex dissipation and to ensure the generation of a well-structured vortex with a high local convective velocity. These three parameters are critical for the generation of a tip vortex which is suitable for interaction experiments.

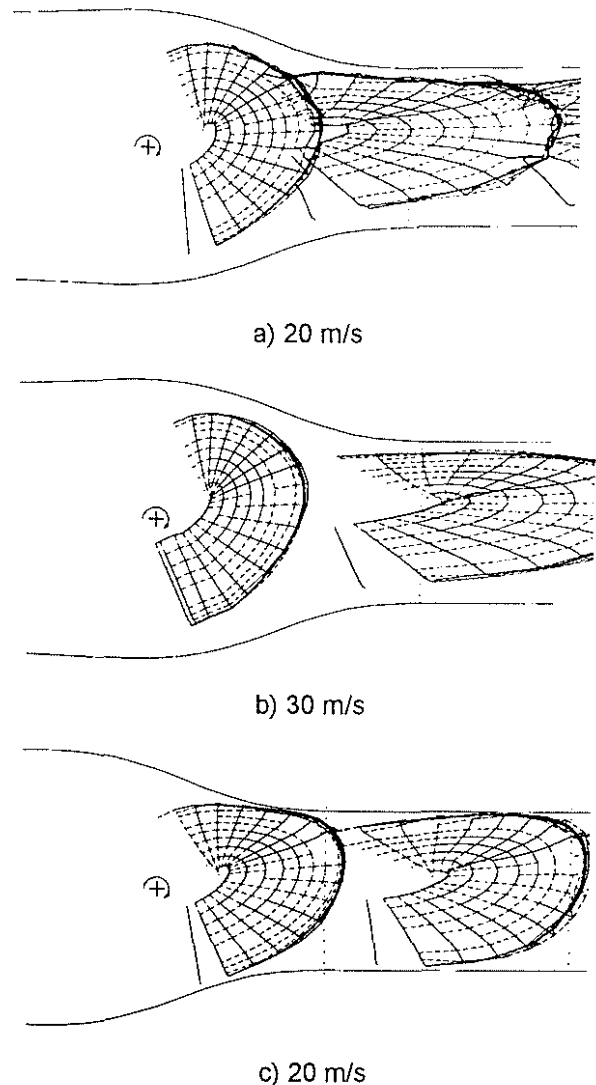
Investigation of the two operating strategies indicated that the optimum theoretical configuration for the generation of a lateral vortex was a single revolution acceleration/deceleration case. To achieve this at even moderate wind speeds necessitated very high rotational accelerations of the blade and, hence, high actuation loads. In fact, these loads were such that design of an appropriate actuation system proved impractical. Attention was, therefore, focused on the continuous running strategy.

Figure 7 depicts three examples of continuous running cases which illustrate some of the effects predicted by the numerical model. In all the cases presented, the rotational speed of the blade is such that the blade tip speed is a constant 50m/s. In Fig. 7a the blade rotational axis is a considerable distance upstream from the working section. The diagram illustrates the distortion that occurs in the wake with the blade at this location in the contraction/settling chamber. As may be observed, lower streamwise velocity in this region of the tunnel necessitates a lower tip speed to avoid interaction of consecutive wakes.

An increase in wind tunnel velocity to 30 m/s is illustrated in Fig. 7b. It is interesting to note that each wake structure is now well separated from those around it but its general form is still unacceptable because of the high curvature of the vortex system in the working section.

Figure 7c illustrates the optimum continuous running case examined in this study. As in Fig. 7a the wind tunnel velocity is 20m/s but this time the rotor hub is located much closer to the working section of the tunnel. This has the effect of reducing the wake curvature and, thus, increasing

the separation distance between consecutive wake structures. In fact, the separation between tip vortices is approximately equal to the length of the working section and is sufficient to measure the vortex trajectory without significant influence from preceding vortical wake structure. For this case, the rotor had a of radius 0.75 metres.



**Fig.7- Illustration of Calculated Rotor Wake Shapes**

Practical consideration must also be given to the proximity of the blade tip to the tunnel wall during the rotation of the blade. The numerical model takes no account of the viscous effects that would be experienced in this region. This is not a feature when the blade crosses the working section, but must be considered when the blade initially pitches up to generate the wake. Viscous interaction with the wall may result in vortex dissipation and produce unwanted phenomena in the convecting vortex structure. If this does occur then alteration of the radius of the blade would probably be required.

The strength of the tip vortex produced by the generator depends, to a large extent, on the pitch profile which the blade is subject to. If this profile is expressed non-dimensionally, the magnitude of the interacting vortex is simply related to the maximum pitch of the blade.

### Experimental Facility and Apparatus

The experiments were conducted in the 1.15m x 0.85m low speed wind tunnel of the Department of Aerospace Engineering, Glasgow University. This is a closed return facility capable of speeds up to 33 m/s. The test section length is 1.8m. The tunnel is equipped with an automated two component traverse which can be wall mounted vertically or on a support structure horizontally. The traverse is actuated via stepper motors controlled through a data acquisition board by software written under Labview. The positional error of the traverse is of the order of 0.5%.

The transverse vortex generator facility consisted of a single, variable pitch, rotating blade with a NACA 0015 cross section, positioned in the wind tunnel contraction (Fig 8). The rotating blade had a rectangular planform of chord 0.1m and tip radius 0.75m from the hub centre (0.66m total blade length). This resulted in a minimum clearance of 0.025m between the rotor tip and the tunnel wall. As discussed previously, these parameters were determined from the numerical model.

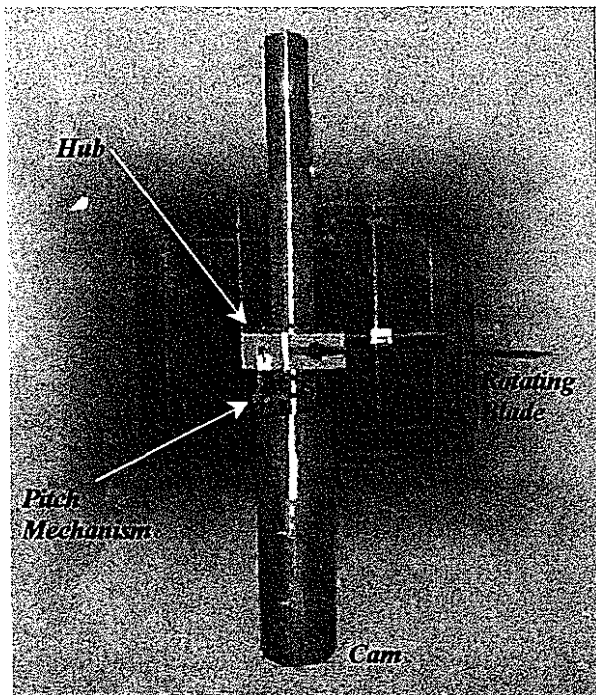


**Fig.8- Illustration of Experimental Set-Up.**

The rotor configuration adopted was that of a rigid blade with no flap and lag hinges. A flap hinge

would have alleviated the root stresses and moments transferred to the hub by allowing out of plane motion. However, the vertical location of the tip could possibly have varied causing the position of the generated tip vortex to be uncertain. Also, if a flap hinge had been employed the motion of the blade would have introduced aerodynamic and inertial forces in the plane of the rotor and so, a corresponding lag hinge would probably have been required (as is the case with helicopter rotors). These hinges would have increased the complexity of the apparatus significantly and therefore the cost. Adaptation of the numerical model may also have to have been made for comparative purposes. In the rigid blade design, the aerodynamic forces generated on the blade were transferred through the hub and shaft to the external support structure.

The required blade pitch profile was produced by a spring-loaded pitch link mechanism connected to a roller which was designed to follow an appropriately shaped non-rotating cam. This cam took the form of a shroud around the lower section of the rotating shaft assembly which was isolated from the rotating shaft and bolted to a mounting plate below the wind tunnel floor. The actual pitch profile was machined along the top edge of the shroud. Thus, as the blade hub rotated, the roller followed the cam profile causing the pitch link to be displaced vertically which, in turn, produced the pitching motion of the blade.

The cam profile was such that zero degrees blade incidence, occurred when the blade was pointing into the settling chamber (45 degrees azimuthal travel on either side of the centre line). In this phase, the roller was at its lowest position. In the next 90 degree phase of motion, the blade was pitched up to 10 degrees. In this phase, the constraining arm and pitch arm return to the horizontal and the spring internally housed in the hub is compressed. After this, the blade crossed the working section at a constant incidence of 10 degrees (azimuthal position 45 degrees either side of the centre line). In the final 90 degree phase, the blade returned to zero degrees. In this phase, the spring forced the roller to remain in contact with the cam. Due to the roller being 90 degrees ahead of the rotating blade, the cam was necessarily 90 degrees out of phase with the blade.

The rotor rig was equipped with two sensors. The first optical sensor provided a measurement of the rpm of the rotating blade to enable the rotational speed of the blade to be controlled. The second sensor provided an external trigger for the hot-wire system via a 16 channel BNC input board for the internal A/D Converter.

Measurements of the magnitude and associated direction of the time-dependent velocities, produced in the wind tunnel working section by the wake passage, were obtained using a cross-wire probe connected to a TSI IFA-300 three-channel constant temperature anemometer system. For a single cross-wire, the maximum sampling rate for this system is 400 kHz. The cross-wire probes used in this study were DANTEC 55P61 probes. The sensor wires on these probes are 5mm diameter platinum plated tungsten wires with a length/diameter ratio of 250, which form a measuring volume of approximately 0.8mm in diameter and 0.5mm in height. The wires are orientated perpendicular to each other corresponding to 45 degrees from the freestream direction which gives the best angular resolution. An additional temperature probe was used to correct the anemometer output voltages for any variation in ambient flow temperature.

For probe calibration, an open jet vertical wind tunnel with a maximum operating velocity of 43 m/s was used. A support allowed the sensors of X-wire probe to be rotated by 30 degs in the plane of the sensors. Variation of the flow velocity and yaw angle then enabled the coefficients of the effective velocity method to be determined.

### Description of Tests

The main variables in the tests conducted were the working section velocity and rotor rotational speed. In addition the measurement position, sampling time and sampling frequency were also varied. However, a constant sampling frequency of 5000 Hz and a sampling time of 0.8 seconds was used for the majority of tests. All tests reported here were conducted with the x-wire probe situated 1.65 m downstream of the rotating axis.

Table 1 details the initial tests which were conducted at the two extremes of the operating range to investigate the actual existence of a periodic signal representative of a transverse vortex. Tests 1 and 2 were conducted at low working section velocity and rotational speed settings (10 m/s and 400 rpm respectively) and tests 3 and 4 at high wind tunnel and rotational speed settings (20 m/s and 520rpm (test3), 600 rpm(test4)). All measurements were made at position 30mm to the right of the wind tunnel centre line (when looking upstream into the settling chamber). This position was largely free of disturbances produced in the wake of the rotor hub. The vertical position of the probe was determined by traversing the probe vertically until a signal indicative of a vortex was detected. The position corresponding to the maximum response

varied, as would be expected, with the operating parameters of the rig. For consistency between tests, however, a fixed location 30mm below the rotor plane was used.

Table 1 – Initial test cases conducted.

Test Case	Freestream Velocity (m/s)	Rotational Speed (rpm)	Sampling Time (secs)
1	10	400	0.4
2	10	400	0.8
3	20	520	0.4
4	20	600	0.8

A further series of tests were conducted at a constant working section velocity of 10 m/s. In these tests, the relationship between the rotational speed setting and the periodic nature of the convecting vortex was investigated as was the dependency of the measured signal on the horizontal measurement location. These tests were then repeated for working section velocities of 20 and 15 m/s.

All the tests documented here used a manual trigger to obtain a time history containing the signature of several vortex systems. These were sufficient to both identify and document the characteristics of the periodic vortex passage.

### Discussion of Experimental Results

The hot-wire results are presented in this section in the form of time series for the streamwise ( $u$ ) and the vertical ( $v$ ) velocity components. Figure 9 illustrates the orientation of the probe in relation to a convecting vortex when looking horizontally through the working section and indicates the associated sign convention used for the velocity components.

In Fig. 10a, the streamwise and vertical velocity time series for Test 1 are presented. As can be seen, there is a strong periodic signal indicative of a vortex in both time series, with three vortices evident in the 0.4 second sample time. The period between each vortex is approximately 0.15 seconds which corresponds exactly to the prescribed rotational speed of 400 rpm. This corresponds to a vortex spacing of 1.5m.

The first two vortex passes are characterised by a sharp rise in the measured streamwise velocity component as the vortex approaches the probe. Subsequently, the velocity peaks and then returns to the freestream level as the vortex moves downstream of the probe. In both cases, the peak

in the streamwise velocity component is coincident with a sign change in the vertical component.

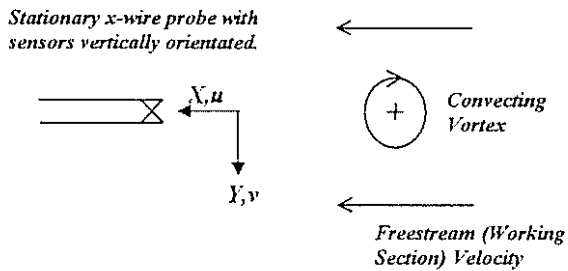


**Fig.9- Illustration of probe orientation with respect to convecting vortex.**

As may be observed in Fig.9, if the vortex were to pass above the probe, the superposition of the freestream velocity with the induced velocity from the convecting vortex would result in the observed sharp increase in streamwise velocity as the vortex passes the measurement location. This increase would reach a maximum value if the vortex were to pass exactly one core radius above the probe. If, on the other hand, the probe were to move upwards into the vortex core, the magnitude of the response of the streamwise velocity would decrease rapidly. Continuing this trend, if the vortex were to pass below the probe, the response of the streamwise velocity component would reverse to become a decrease in velocity.

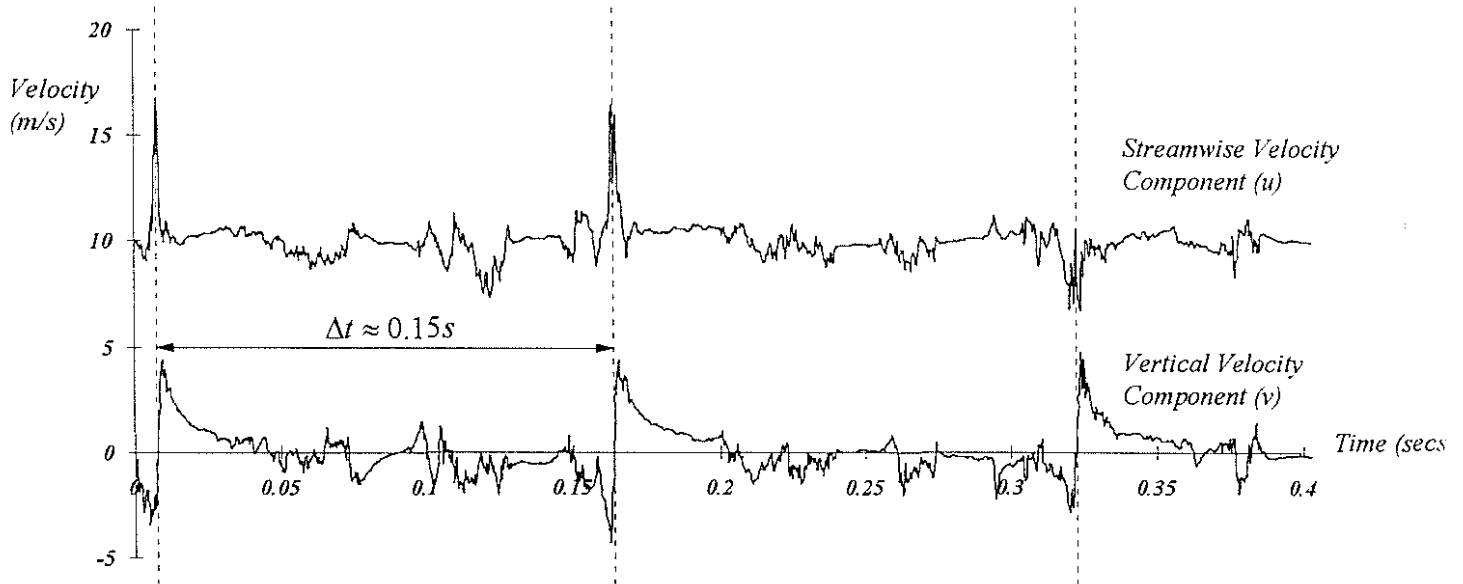


**Figure 10a – Time series for initial test case 1 depicting the periodic convecting vortex.**

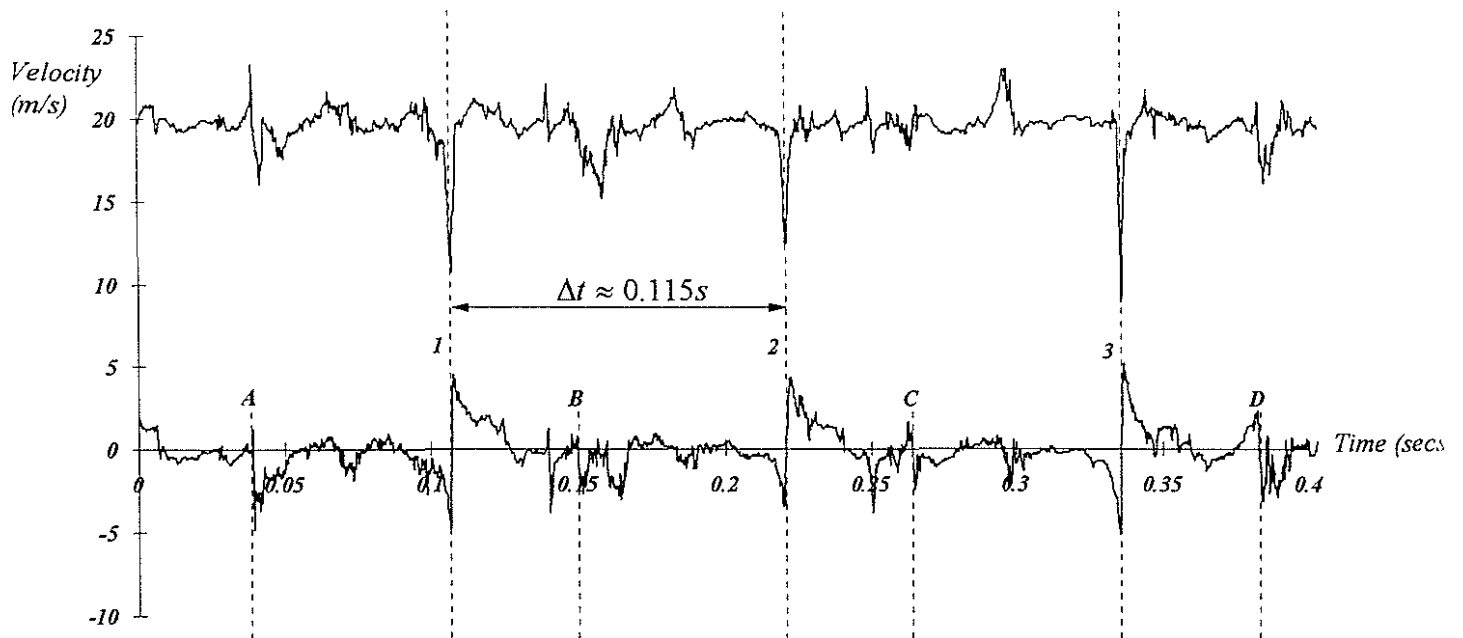


**Figure 10b – Time series for initial test case 3 depicting the periodic convecting vortex.**

In contrast to the above, the expected response of the vertical velocity component depends only on the distance of the probe from the vortex centre. As the probe is moved out from the vortex centre, the peak to peak change measured during the vortex passage would gradually decrease. This trend would continue up to and beyond the edge of the vortex core.

Given the expected behaviour of the two velocity components, it is possible to formulate an explanation for the measured response during the passage of the third vortex in Fig. 10a. The streamwise response is consistent with the vortex passing below the probe by an amount greater than the vortex core radius. Consequently, the magnitude of the vertical velocity change is slightly smaller than the previous cases.

In Fig. 10b, the freestream velocity has been increased to 20 m/s which was the maximum design speed of the facility. The rotational speed of the blade has also been increased to a value of 520 rpm. Again, the period between convecting vortices (0.115 secs) is consistent with the rotational speed of the blade. This figure depicts three convecting vortices, numbered 1, 2 and 3, which, due to the greater downwash from the rotor, pass below the probe. In addition, however, there appears to be a second weak periodic signal between each vortex pass. This signal is characteristic of a vortex of the opposite sign to the strong transverse tip vortex and is identified in the figure by the letters A, B, C and D. As may be observed in Fig. 7c, which is a similar case calculated using the numerical model, there is a strong root vortex which exists to the right of the centre line; In Fig. 7, the vortex strength is indicated by the line thickness. This corresponds to the same location as the measurement probe and so this second periodic signal could be a rolled up root vortex. The response, however, could also be due to a coalescing of the shed vorticity produced during the pitching of the rotor blade. More detailed tests would be required to fully investigate the operating conditions which generate this secondary periodic signal and the measurement locations where it is evident. However, this may be complicated by the fact that this weak signal is clearly severely affected by turbulence.

The results presented above are illustrative of the basic features apparent in all of the measured hot-wire signals. In each case, the measurements, confirmed the findings of the earlier numerical study in terms of vortex position and phasing. Generally, as may be expected, the clearest and most consistent vortex signatures were obtained at the highest rotor speeds. As indicated in the numerical study, this is consistent with the production of a wake geometry suitable for

interaction experiments, when the rotor is in its optimum position.

## **Conclusions and Future Work**

The new vortex generator facility has proved to be successful in the generation of a transverse vortex which convects through the working section of a low speed wind tunnel. It is, therefore, intended to use this technique for an experimental investigation into Blade Vortex Interaction with the vortex orthogonal to the plane of the aerofoil.

The next phase of the work will involve interacting the convecting vortex with a stationary blade located in the working section of the wind tunnel used for the present study. This blade will be instrumented with miniature pressure transducers to measure the change in surface pressure distribution during the interaction. In addition, hot-wire measurements will be made in the vicinity of the blade surface to measure the distortion of the vortex as it passes the blade.

Following this, the new vortex generation technique will be implemented in the larger 2.6mx2.1m low speed wind tunnel at Glasgow University. Once installed, the generator will be used for interaction studies on a stationary blade which will be instrumented with a large number of surface pressure transducers. Then, the stationary blade will be replaced by a tail rotor model which will have, in addition to basic force instrumentation, blades fitted with miniature pressure transducers. These two test programmes should make a significant contribution to contemporary understanding of both the pure orthogonal interaction and the more complex interactional environment of the tail rotor. The work should also compliment research planned at DERA within the HELIFLOW project to investigate quartering flight. This will use the DERA Mach scaled rotor rig together with a new tail rotor model.

## **Acknowledgements**

The authors would like to acknowledge the support of the British Ministry of Defence through the Defence Evaluation Research Agency (DERA). The work was funded by the DERA under extra-mural agreement ASF/2163U.

## **References**

1. Ellin A.D.S., "An In-Flight Investigation of Lynx AH Mk5 Main Rotor/Tail Rotor Interactions", 19th European Rotorcraft Forum, Cernobbio, Italy, Sept. 1993.

2. Wiesner W., Kohler G., "Tail Rotor Performance in Presence of Main Rotor, Ground and Winds", 29th Ann. Forum of the Amer. Heli. Soc., May 1973.
3. Leverton J.W., Pollard J.S., Wills C.R., "Main Rotor Wake/Tail Rotor Interaction", 1st European Rotorcraft & Powered Lift Forum, Sept 1975.
4. Lawson M.V., "Progress Towards Quieter Civil Helicopters", Aero. J., 209-23, June/July 1992.
5. Sternfeld H., "Recent Developments in Helicopter Noise Reduction", 11th Congress of the International Council of the Aero. Sciences, Lisbon, Sept. 1978.
6. Tyler D.J., Vincent A.H., "Future Rotorcraft Technology Developments", Aero. J., 451-60, Dec. 1996.
7. Sheridan P.F., Smith R.P., "Interactional Aerodynamics - A New Challenge to Helicopter Technology", 35th Ann. Forum of the Amer. Heli. Soc., May 1979.
8. Booth E.R., Yu J.C., "Two Dimensional Blade-Vortex Interaction Flow Visualisation Investigation", AIAA Paper 84-2307, Oct. 1984.
9. Booth E.R., "Surface Pressure Measurement During Low Speed Two-Dimensional Blade-Vortex Interaction", AIAA Paper 86-1856, July 1986.
10. Booth E.R., Yu J.C., "New Technique for Experimental Generation of Two-Dimensional Blade-Vortex Interaction at Low Reynolds Number", NASA TP-2551, March 1986.
11. Straus J., Renzoni P., Mayle R.E., "Airfoil Pressure Measurements During a Blade-Vortex Interaction and a Comparison with Theory", AIAA Paper 88-0669, Jan. 1988. (Also AIAA J. 28, 222-8, Feb. 1990)
12. Homer M.B., Saliveros E., Galbraith R.A.McD., "An Experimental Investigation of the Oblique Blade-Vortex Interaction", 17th European Rotorcraft Forum, Berlin, Germany, Sept. 1991.
13. Homer M.B., Stewart J.N., Galbraith R.A.McD., Grant I., Coton F., Smith G.H., "Preliminary Results from a Particle Image Velocimetry Study of Blade-Vortex Interaction", 19th European Rotorcraft Forum, Cernobbio, Italy, Sept. 1993.
14. Homer M.B., Stewart J.N., Galbraith R.A.McD., Grant I., Coton F., "An Examination of Vortex Deformation during Blade-Vortex Interaction Utilising Particle Image Velocimetry", 19th Congress of the International Council of the Aero. Sciences, Anaheim, California, Sept 1994.
15. Coton F.N., De la Iglesia F., Galbraith R.A.McD., Horner M.B., "A Three-Dimensional Model of Low Speed Blade-Vortex Interaction", 20th European Rotorcraft Forum, Amsterdam, The Netherlands, Oct 1994.
16. Jones, H.E., Caradonna, F.X., "Full Potential Modelling of Blade Vortex Interactions", Vertica, Vol. 12, pp 129-145, 1988
17. Srinivas V., Chopra I., Haas D., McCool K., "Prediction of Yaw Control Effectiveness and Tail Rotor Loads", 19th European Rotorcraft Forum, Cernobbio, Italy, Sept. 1993.